As of 10 June 2016

This GOES-R Level 2+ space weather Algorithm Theoretical Basis Document (ATBD) is preliminary and subject to change as the GOES-R Program prepares for a launch in late 2016.

The NOAA National Centers for Environmental Information (NCEI) is currently developing a demonstration version of the Satellite Product Analysis and Distribution Enterprise System (SPADES) which will host the L2+ algorithms. The operational SPADES will be instantiated by the National Weather Service in FY2017 to serve the needs of the Space Weather Prediction Center (SWPC).

Updated versions of the L2+ ATBDs will periodically be made available and posted to the SPADES website.

Bill Denig
NCEI

http://www.ngdc.noaa.gov/stp/space-weather/online-publications/stp_sii/spades/

NOAA NESDIS CENTER for SATELLITE APPLICATIONS and RESEARCH

GOES-R XRS.07 ALGORITHM THEORETICAL BASIS DOCUMENT
Version 1.2

Hardcopy Uncontrolled

TITLE: XRS.07 ALGORITHM THEORETICAL BASIS DOCUMENT VERSION 1.2

AUTHORS:
S. Dave Bouwer
Donald Woodraska
Steven Mueller
Tom Woods
Frank Eparvier
Kent Tobiska

APPROVAL SIGNATURES:

_____<Actual Signature Date>
<Name of Technical Approver> Date
Technical Approver

_____<Actual Signature Date>
<Name of Agency Approver> Date
Agency

XRS.07 ALGORITHM THEORETICAL BASIS DOCUMENT VERSION HISTORY SUMMARY

Version	Description	Revised Sections	Date
1.0	First draft, Dave Bouwer, SET	All	1 Mar 2011
1.1	Draft for CDR	All	21 Jul 2011
1.2	Modified FLARE_END definition, added integrated flux at EVENT_END, content refinements	All	31 Aug 2011

TABLE OF CONTENTS

LIST OF FIGURES 9

ABSTRACT 12

1.0 INTRODUCTION 13

1.1 Purpose of This Document 13
1.2 Who Should Use This Document 13
1.3 Inside Each Section 13
1.4 Related Documents 14
1.5 Revision History 14

2.0 OBSERVING SYSTEM OVERVIEW 14

2.1 Preliminary Design Requirements 17
2.1 Products Generated 19
2.1.1 Real-time Event Table 19
2.1.1 Post-Event Table Product 22
2.2 Instrument Characteristics 23

3.0 ALGORITHM DESCRIPTION 24

3.1 Algorithm Overview 25
3.2 Processing Outline 26
3.2.1 Mitigating Signal Noise and False-Positives 28
3.3 Algorithm Input 29
3.3.1 Primary Sensor Data 29
3.3.2 Configuration Parameters 29
3.4 Theoretical Description 30
3.4.1 Physics of the Problem 31
3.4.2 Mathematical Description 31
3.4.3 Algorithm Output 34

4.0 TEST DATA SETS AND OUTPUTS 35

4.1 Simulated/Proxy Input Data Sets 35
4.2 Output from Simulated/Proxy Inputs Data Sets 35
4.2.2 Error Budget 38

5.0 PRACTICAL CONSIDERATIONS 39

5.1 Numerical Computation Considerations 39
5.2 Programming and Procedural Considerations 40
5.3 Quality Assessment and Diagnostics 40
5.4 Exception Handling 41

5.5 Algorithm Validation 41

6.0 ASSUMPTIONS AND LIMITATIONS 41

6.1 Performance.....42
6.2 Assumed Sensor Performance.....42
6.3 Pre-Planned Product Improvements 42

7.0 REFERENCES 42

LIST OF FIGURES

Figure 1. GOES-14 0.1-0.8 1-minute X-ray Flux during solar maximum conditions....15
Figure 2. One-minute, hourly average, and daily background flux near Solar Cycle 23 maximum. 17
Figure 3. An example of the algorithm's performance in detecting events. 21
Figure 4. XRS solar diodes configuration. 24
Figure 5. XRS.07 Algorithm Flowchart Overview. 27
Figure 7. Event identification concept. 32
Figure 8. Example of algorithm performance in detecting flares, Nov. 6, 2010 ...36

LIST OF EQUATIONS

Equation 1. The first equation used to detect the onset of a flare. 32
Equation 3. The exponential model used to indentify the start of the impulsive phase of a flare. 33
Equation 4. The equation used to identify a flare event end. 33
Equation 5. Determining the percent increase of the exponential fit. 34

LIST OF TABLES

Table 1. NOAA flare classifications 16
Table 2. NOAA SWPC X-ray warning and alert scale 16
Table 3. XRS.07 design goals. 18
Table 4. XRS.07 product data: Event Status Flags. 20
Table 5. The Real-time Event Table Output Product. 22
Table 6. A Event Status Output Table example product. 23

Table 7. Recommended Configuration Parameters.....30

Table 8. Study epochs used for development and testing. 35

Table 9. Real-time Status Output Table example. 37

Table 10. Event Status Output Table example. 38

Table 12. Error budget estimates, assuming a 9-minute data-frame size.....38

LIST OF ACRONYMS

ATBD	Algorithm Theoretical Basis Document
AWG	Algorithm Working Group
CIRES	Cooperative Institute for Research in Environmental Sciences
UTC	Coordinated Universal Time
ISO	International Organization for Standardization
LASP	Laboratory for Atmospheric and Space Physics
NGDC	National Geophysical Data Center
NWS	National Weather Service
SET	Space Environment Technologies
STAR	Center for Satellite Applications and Research
SWPC	Space Weather Prediction Center
XRS	X-ray Sensor

ABSTRACT

This document describes the XRS.07 algorithm that detects X-ray flare events in time series of the XRS 0.1 – 0.8 nm 1-minute average flux. The logical flow of the algorithm is outlined, including error handling methods, how validation using proxy data sets will be accomplished, and explanations of assumptions.

1.0 INTRODUCTION

1.1 Purpose of This Document

The purpose of this document is to provide product developers, reviewers, and users with a theoretical description (scientific, algorithmic, and mathematical) of the GOES-R XRS.07 Flare Event Detection algorithm. This document will describe the design and development of the XRS.07 algorithm, which will ingest 1-minute 0.1-0.8 nm X-ray averages in real time, returning the time at which a flare is detected, when it reaches it maximum, the time at which the flare has decreased to one-half its maximum, and when a flare reaches its pre-flare background. This document provides the operational requirements for this product and defines how these requirements are met with this algorithm. The algorithm inputs, processing, and outputs are described in enough detail to design, develop, test, and implement the necessary processing software.

1.2 Who Should Use This Document

The members of the Space Weather Forecast Office and the Research and Customer Requirements Section of the SWPC should use this ATBD to verify that their operational requirements are being met by the proposed algorithm. They should also use it to understand the strengths and weaknesses of the algorithm as well as its accuracy and applicability. The STAR AIT group should use this document to integrate the algorithm into their collaborative framework environment. It should also be used by the ground segment contractor to design, develop, test, validate and implement the algorithm into the final operational processing system.

1.3 Inside Each Section

Section 2.0 OBSERVING SYSTEM OVERVIEW:
Describes the GOES-R XRS instrument and the measurements that serve as input to the algorithm.

Section 3.0 ALGORITHM DESCRIPTION:
Describes the development, theory, and mathematics of the XRS.07 algorithm. Describes the logical flow of the algorithm, including input and output flow.

Section 4.0 TEST DATA SETS AND OUTPUTS:

Describes the test data sets used to characterize the performance of the algorithm and the data product quality. Describes the results from the algorithm processing on the input data.

Section 5.0 PRACTICAL CONSIDERATIONS:
Discusses issues involving numerical computation, programming and procedures, quality assessment, diagnostics, and exception handling.

Section 6.0 ASSUMPTIONS AND LIMITATIONS:
Describes assumptions made in the implementation of the Flare Event Detection algorithm, and assumptions made in validation, testing, and error handling of the algorithm.

Section 7.0 REFERENCES:

1.4 Related Documents

"GOES-R Series Acronym & Glossary Document", DOC/NOAA/NASA (GOES-R Program/Code 417), P417-R-LIST-0142, July 9, 2008.

"XRS.07 Algorithm Preliminary Requirements Review" (XRS07_PrelimReqReview_db_v3.ppt.pdf), 25 Feb 2011.

1.5 Revision History

Version 1.0 July 21, 2011. S. Dave Bouwer, First Draft.

2.0 OBSERVING SYSTEM OVERVIEW

The GOES XRS measurements have been a crucial component of space weather since 1975, providing an accurate measurement of geo-effective X-ray irradiance from second-to-second real-time conditions to solar-cycle time scales. The integrated 0.1–0.8 nm irradiance is the definitive metric for solar flare classifications, and is a keystone in SWPC operations.

In this document, the terms "event" and "flare" can be used interchangeably. However, a "flare" has specific classifications for forecast operations associated with it (i.e., B, C, M, and X-class flare classifications). The more general "event"

refers to the time series properties, i.e., the beginning, maximum and event end. In both cases, there are solar active region phenomena well represented by the 0.1-0.8 nm X-ray data. **Figure 1** illustrates the typical flare activity during very high levels of solar activity, during which a multitude of flares occur in rapid succession.

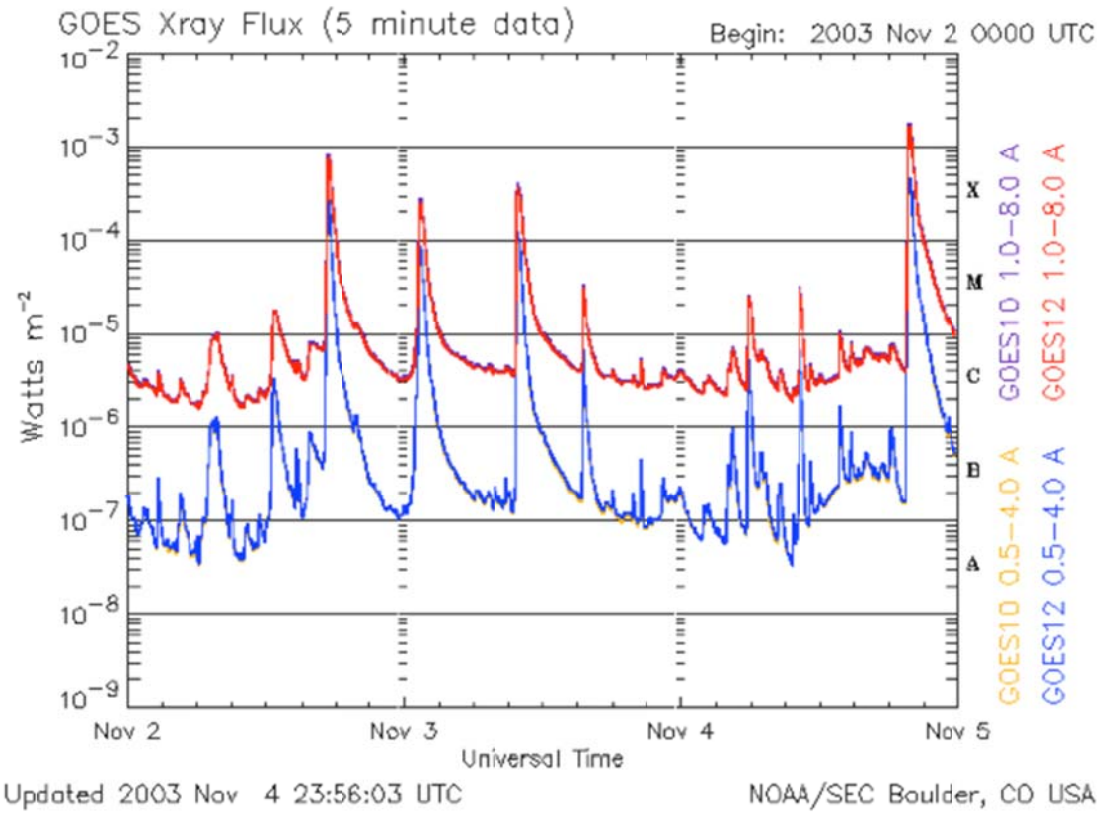

Figure 1. GOES-14 0.1-0.8 1-minute X-ray Flux during solar maximum conditions

The XRS.07 algorithm is primarily designed to be used by forecasters in NOAA/SWPC operations. A vital service the forecast center provides is the early detection of solar flares, which effects HF radio communications and other technologies. NOAA/SWPC has long officially classified flares according to the schema shown in **Table 2**. These classifications are subsequently used by

forecasters to issue alerts and warnings in real-time operations, as well as for post-event analysis.

Table 1. NOAA flare classifications

Flare Classification	0.1-0.8 nm X-ray Flux Level
A – class	Xray flux exceeded 1 x 10^{-8} W/m^2
B – class	Xray flux exceeded 1 x 10^{-7} W/m^2
C – class	Xray flux exceeded 1 x 10^{-6} W/m^2
M – class	Xray flux exceeded 1 x 10^{-5} W/m^2
X – class	Xray flux exceeded 1 x 10^{-4} W/m^2

Additionally, NOAA has standardized another scale to be used for issuing public alerts and warnings, which is consistent with other NWS extreme weather events alerts and warnings. **Table 2** is the basis for warnings and alerts issued by SWPC based on the GOES 0.1 – 0.8 nm x-ray flux measurements.

Table 2. NOAA SWPC X-ray warning and alert scale

NOAA Scale	X-ray Flux Alert and Event Summaries
R1 - Minor	Xray Event exceeded M1 (1 x 10^{-5} W/m^2)
R2 - Moderate	Xray Event exceeded M5 (5 x 10^{-5} W/m^2)
R3 - Strong	Xray Event exceeded X1 (1 x 10^{-4} W/m^2)
R4 - Severe	Xray Event exceeded X10 (1 x 10^{-3} W/m^2)
R5 - Extreme	Xray Event exceeded X20 (2 x 10^{-3} W/m^2)

This scale is useful for adding a criteria in the event detection algorithm. It is known from prior analysis (e.g., GOES_XRS_09_Test_Plan_v2.0b 2010, and SET Technical Report SET_TR2006-002, 2006) that the daily background never exceeds 1 x 10^{-5} W/m^2. Furthermore, an analysis of Solar Cycle 23 indicates nearly no instances where the hourly average flux exceeds 1 x 10^{-4} W/m^2 (an exception is during the April 2001 epoch). Figure 2 illustrates this in the middle panel during April-Oct 2001 epoch (the top panel are 1-minute averages, and the bottom panel the daily background).

This suggests in the XRS.07 algorithm a flux level of 5 x 10^{-5} W/m^2 (corresponding to an R2 Moderate Alert) is a logical level to flag the start of a flare, irrespective of the percentage increase above a background value or other event flags. This is consistent with SWPC operations, and helps ensure all flares above an R2 alert are identified, although it does not guarantee the flare will be detected in the early stages of it's evolution.

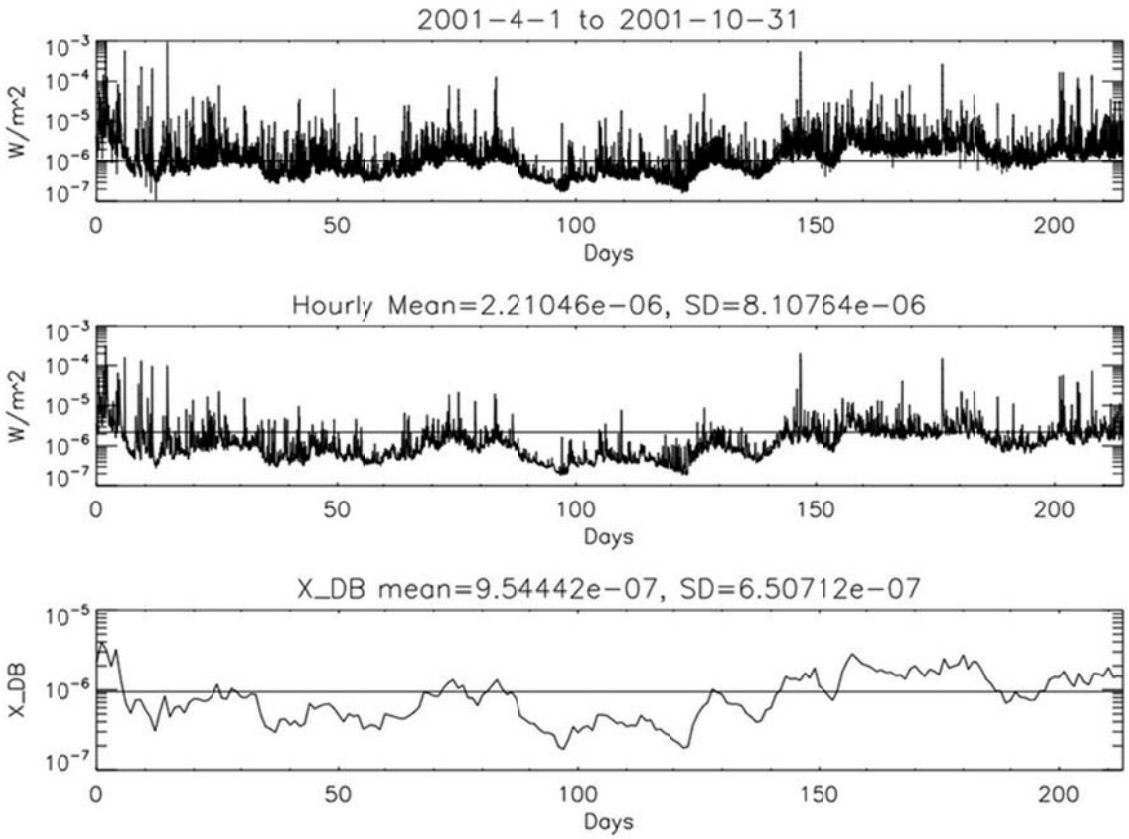

Figure 2. One-minute, hourly average, and daily background flux near Solar Cycle 23 maximum.

2.1 Preliminary Design Requirements

Since 1995 SWPC has been using a flare detection algorithm developed at SWPC (formerly SEL). The primary goal of the algorithm was to detect a flare automatically - as early as possible – at the early start of a flare, so that an automated alert can be directed to the forecasters on duty at the SWPC forecast center. This information is useful for forecasters in issuing alerts and warnings.

NOAA/SWPC currently uses the 1995 flare event detection algorithm in operations, but it is a “legacy” algorithm developed over 15 years ago, and often results in missed events, false-positives, etc., and often requires operator intervention to adjust the flare characteristics post-event. The goal is to significantly improve the current algorithm, achieving much higher percentages in successfully detecting M, C, and X-class flares. Table 3 summarizes the

specification from a NOAA algorithm design review addressing the XRS.07 algorithm requirements.

In an January 2011 Preliminary Design Review, NOAA indicated that the Measurement Accuracy and the 4-minute Temporal Coverage event latency are approximations, and that these requirements may need to be adjusted to reduce the number of false-positive events reported by the algorithm for maximum algorithm performance.

Table 3. XRS.07 design goals.

Specific Inputs	Description	Measure-ment Range	Measure-ment Accuracy	Refresh Rate	Data Latency	Temporal Coverage Qualifier
Level 3 (1 min avg.)	Determining timing and magnitude of x-ray flares from 1 minute averaged data. Event detection needs to work in real time so that the detection of the event is generated and available typically before the event maximum and certainly before the event end	XRSA: $1x10^{-7}$ to $1x10^{-3}$ W/m^2	Accurate Flare Detection 80% for B flares 90% for C flares 99% for M and X flares (TBR)	1 min	1 min	Initial event detection within 4 min of start of event (TBR)

One thing not discussed in the design requirements is the issue of false-positives, i.e., what percentage of flares the algorithm flags as starting, which do not subsequently reach a B-class flare or greater. Or, for example, many B-class flares only reach the criteria for a flare for 1-3 minutes, and subsequently quickly decay back to background in another 1-3 minutes. Additionally, when there is a poor signal-to-noise ratio, a sudden increase in the data may only represent instrument noise. This scenario is often present during low levels of solar activity.

However, the issue of false-positives is clearly a design consideration: an excessive number of false-positives have little operational or scientific value.

2.1 Products Generated

The algorithm produces two outputs associated with the event detection: A Real-Time Event Output Table updated every minute with the current event properties, and a Event Status Output Table, which only contain event properties at the time they actually occurred, thus there are latencies when the table is updated. The Real-Time Event Output Table will be used in real-time forecast operations, where rapid flare detection and minute-to-minute status information is the priority. The Event Status Output Table is designed more for post-event analysis, where the flare is more accurately characterized. This table can have a number of practical and scientific applications, such as determining the total energy input to the ionosphere's D-region.

2.1.1 Real-time Event Table

The XRS.07 algorithm must detect X-ray flares in real-time operations, so that the detection of the event is generated and available typically before the event maximum and certainly within 1-5 minutes of flare maximum. A Real-Time Event Output Table will be maintained by the XRS.07 algorithm for use by forecasters in operations.

Thus the following data illustrated in **Table 4** will be included in the XRS.07 X-ray flare event detection product. The Event Status Flags accompany the data output every minute. When the algorithm is first initiated and no earlier data is available, the algorithm enters an "MONITORING" (T_M) state, and will not change until an event has begun, at which point an "EVENT_START" (T_S) is set.

The "EVENT_START" (T_S) corresponds to a specific time at which the algorithm has detected a certain percentage rise above the background and other criteria specific to a flare are met, and it is probable that a solar flare has begun. After this status value is entered in the output table, the algorithm enters an "EVENT_RISE" (T_R) condition, and this value is repeated each minute until the flare reaches it's maximum and the "EVENT_PEAK" (T_P) status is set.

After T_P is reached, the algorithm repeats the "EVENT_DECLINE" (T_D) status value each minute until the EVENT_END (T_E) has been detected, or a new flare

has started before reaching T_E. Once T_E has been reached, the algorithm repeats the "MONITORING" (T_M) status value until an new flare has begun.

Not uncommon is a data outage period, such as during eclipses. In this case, an "IMPAIRED" (T_I) status flag is set. The algorithm will maintain this status value until there are sufficient data for the algorithm to perform calculations, at which point the algorithm will set the status flag to MONITORING.

But in many cases, after T_E has been reached, the flare may continue to decline to a background value measured just prior to the start of the event. This "POST_EVENT" (T_B) event condition provides a means to characterize the integrated flux and flare evolution characteristics of a flare, and this information has useful scientific value.

The Event Flag integer in **Table 4** is for convenience in coding algorithms that read the output table to assign event status flags.

Table 4. XRS.07 product data: Event Status Flags.

Symbol	Value	Note	Event Flag
T_M	MONITORING	There is no event in progress; data is near background levels.	1
T_S	EVENT_START	A flare has started; the flux has risen above the background (impulsive phase).	2
T_R	EVENT_RISE	A flare has started, but the flare maximum has not been reached (impulsive phase).	3
T_P	EVENT_PEAK	The flare maximum has been reached.	4
T_D	EVENT_DECLINE	The flare has begun to decay (gradual flare phase)	5
T_E	EVENT_END	The flare has decayed to ½ of flare maximum	6
T_B	POST_EVENT	The flare has decayed to the pre-flare background	7
T_I	IMPAIRED	The algorithm has detected missing data within a data frame and there are insufficient data to determine the status. After sufficient data is available, the algorithm will set the MONITORING event status.	0

Figure 3 below illustrates how these Status Values are applied. In the figure, the vertical line, corresponding to EVENT_START, marks the time the algorithm detects an event start. The EVENT_PEAK is indicated by a square, the EVENT_END by an X, and the POST_EVENT by a triangle. For example, the first small flare near 01 UT shows all these event components. There is a complex event beginning near 13:00 UT, which contains several event starts in rapid succession due to the complex structure of the flare. These details will be discussed in greater detail later in this document.

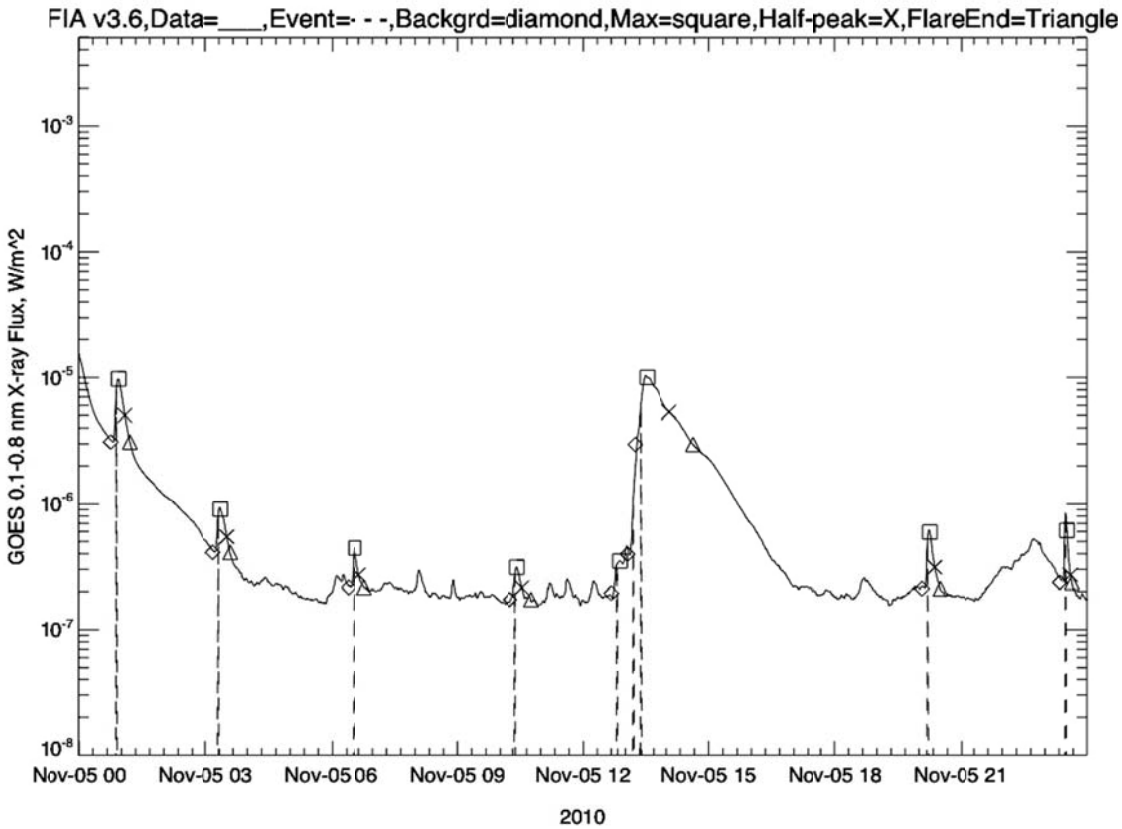

Figure 3. An example of the algorithm's performance in detecting events.

Table 5 illustrates the real-time table updated every minute by the algorithm. Focusing on the first small flare near 01 UT one can see the event start, peak, decline, and flare end status values in the span of 20 minutes. In this example, configuration parameters were set to be very sensitive to rapidly detecting any flares.

Table 5. The Real-time Event Table Output Product.

YYYY	MM	DD	HH	MM	JD	FLUX	Event_Status
2010	11	05	00	50	2455505.534722	3.564E-06	EVENT_DECLINE
2010	11	05	00	51	2455505.535417	4.572E-06	EVENT_DECLINE
2010	11	05	00	52	2455505.536111	6.230E-06	EVENT_START
2010	11	05	00	53	2455505.536806	7.966E-06	EVENT_RISE
2010	11	05	00	54	2455505.537500	9.134E-06	EVENT_RISE
2010	11	05	00	55	2455505.538194	9.659E-06	EVENT_RISE
2010	11	05	00	56	2455505.538889	9.724E-06	EVENT_RISE
2010	11	05	00	57	2455505.539583	9.383E-06	EVENT_RISE
2010	11	05	00	58	2455505.540278	8.819E-06	EVENT_RISE
2010	11	05	00	59	2455505.540972	8.212E-06	EVENT_PEAK
2010	11	05	01	00	2455505.541667	7.577E-06	EVENT_DECLINE
2010	11	05	01	01	2455505.542361	6.969E-06	EVENT_DECLINE
2010	11	05	01	02	2455505.543056	6.408E-06	EVENT_DECLINE
2010	11	05	01	03	2455505.543750	5.889E-06	EVENT_DECLINE
2010	11	05	01	04	2455505.544444	5.424E-06	EVENT_DECLINE
2010	11	05	01	05	2455505.545139	5.013E-06	EVENT_END
2010	11	05	01	06	2455505.545833	4.638E-06	MONITORING
2010	11	05	01	07	2455505.546528	4.298E-06	MONITORING
2010	11	05	01	08	2455505.547222	4.008E-06	MONITORING
2010	11	05	01	09	2455505.547917	3.739E-06	MONITORING
2010	11	05	01	10	2455505.548611	3.505E-06	MONITORING
2010	11	05	01	11	2455505.549306	3.285E-06	MONITORING
2010	11	05	01	12	2455505.550000	3.102E-06	POST_EVENT
2010	11	05	01	13	2455505.550694	2.949E-06	MONITORING
2010	11	05	01	14	2455505.551389	2.804E-06	MONITORING

2.1.1 Post-Event Table Product

In addition to a 1-minute cadence of the Real-Time Event Output Table, a Event Status Output Table is updated whenever there is an EVENT_START, EVENT_PEAK, EVENT_END, and POST_EVENT. This table reports the actual times of the event components, not the apparent time the algorithm detects the events when running in real-time (**Table 5**). The Event Status Output Table (**Table 6**) is consistent with the EUVS.04 event detection algorithm, providing a means to compare many solar flare properties over a range of x-ray and EUV wavelengths. This capability has not been available prior to recent GOES and SDO/EVE measurements, but it can provide a more accurate characterization for post-event analysis.

Table 6 below illustrates the columns for the event's start, peak, end, event status, and an auxiliary column used for supplementing event information, particularly the estimated pre-flare background flux (EVENT_START) and flare

class (EVENT_PEAK). The MONITORING, EVENT_RISE, DECLINING, and POST_EVENT statuses contain no auxiliary entries.

Table 6. A Event Status Output Table example product.

YYYY MM DD HH mm	Julian Date	Flux, W/m^2	Event Status	Auxiliary
2011 07 08 11 44	2455750.988889	5.971E-07	EVENT_START	3.546E-07
2011 07 08 11 52	2455750.995833	2.781E-06	EVENT_PEAK	C 2.8
2011 07 08 12 07	2455751.004861	8.912E-07	EVENT_END	4.0132E-5
2011 07 08 12 30	2455751.020833	3.421E-07	POST_EVENT	-

Prior studies of solar x-ray variability and the current analysis show there are many instances where a flare does not end or reach a background level before another flare has begun. A large flare can occur well before a prior flare has decayed to a background level, or even well before the irradiance has fallen to ½ of the flare maximum. Consequently, the conclusion of an event can be either when the irradiance has declined to ½ of the irradiance at the flare peak ("Half-Max" EVENT_START), or when a new flare has begun prior to declining to ½ of the flare peak (EVENT_START). Note that a new flare can begin at any time, event during the evolution of another flare, so there can be more than one EVENT_START at the onset of a new event, especially when there are multiple flares or double-ribbon flares.

2.2 Instrument Characteristics

Prior to GOES-R, the XRS instrument measured X-ray flux using two bandpass channels from a heritage design employing an ion-chamber. These channels are commonly referred to as the XRS-A (0.05-0.4 nm) and XRS-B (0.1-0.8 nm), both of which are in the soft X-ray portion of the electromagnetic spectrum. The ion-chamber design has two limitations: it 'bottom-outs' during low periods of solar activity, and is unable to effectively measure X-ray flux $\Phi < 1.0 \times 10^{-8}$ W/m^2 (approximately), and the instrument becomes saturated during major flares ($\Phi > 1.7 \times 10^{-3}$ W/m^2, approximately).

The primary goal of the re-designed XRS instrument is to continue the XRS measurements in the same spectral channels, while improving on the limitations of the legacy instrument. The new XRS instrument design addresses these limitations, while adding additional capabilities. The changes include using Si photodiodes instead of ionization cells, using multiple channels to allow wider

dynamic range, providing quadrant photodiodes for real-time flare location measurements, and improved detailed calibration using the NIST Synchrotron Ultraviolet Radiation Facility (SURF) in Gaithersburg, Maryland.

The new design will provide irradiance range of more than 6 orders of magnitude by including two photodiode sets covering different portions of the irradiance range for each of the XRS A and B channels, XRS-A1 and XRS-A2, and a similar specification for XRS-B (B1 and B2).

Figure 2 below illustrates the instrument solar diode sensors that measure both the XRS-A and XRS-B channels, in addition to “dark” photodiodes to measure background signal variations, and the quadrant photodiodes for flare location determination. The 1-minute averages of the XRS-B channels will be calculated from the Level 1b data product for use in the Flare Event Detection Algorithm.

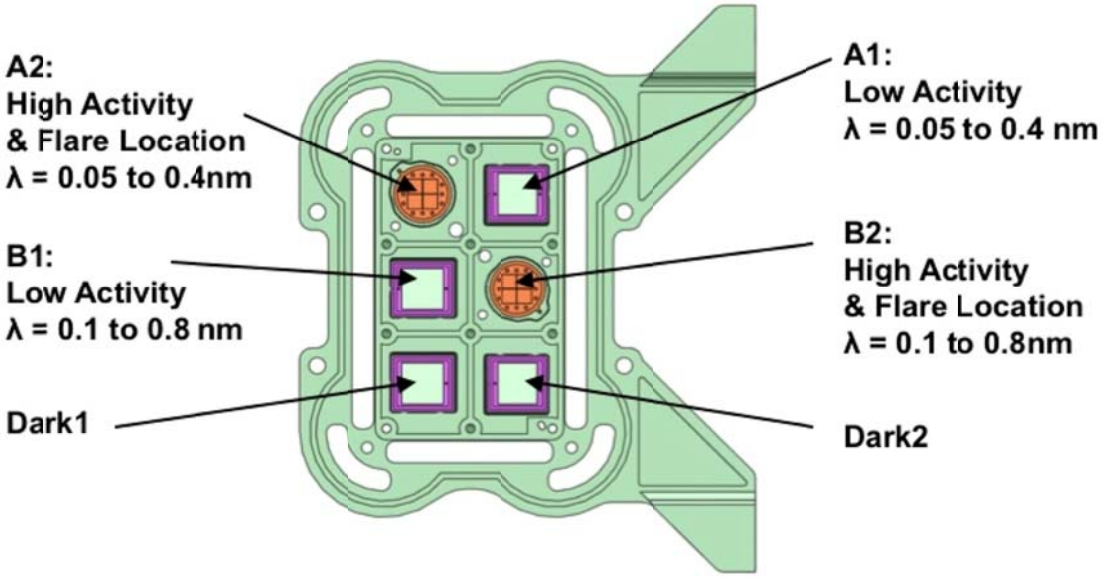

Figure 4. XRS solar diodes configuration.

3.0 ALGORITHM DESCRIPTION

The XRS.07 Flare Event Detection algorithm is intended to be running continuously in SWPC real-time operations. The current flare status (i.e., start, maximum, etc.) will likely be displayed in a forecast center when it is detected, potentially sounding an alarm to alert forecasters of an impending flare.

The XRS.07 Flare Event Detection algorithm will be designed to be robust (i.e., all exception conditions are anticipated and only valid data is passed on), and to achieve the highest possible performance in detecting the majority of B, C, M, and X-class flares.

The algorithm is designed to be a callable routine for increased flexibility and extensibility in final implementation. It is expected it will be run continuously, and will demonstrate no “memory leaks” or other computational exceptions resulting in failure or errors. In other words, the algorithm is designed with a “Trust, but verify” philosophy to ensure maximum fault-tolerance.

The algorithm will initially be written in the ITT/IDL (Interactive Data Language), to develop the initial logic and data plots. However, the XRS.07 code will be delivered in the Fortran programming language, once the final design is established.

3.1 Algorithm Overview

The algorithm will be a callable subroutine or object, so it is assumed the caller of the subroutine will provide it input of the historical or near real-time data in data tables or a similar data array structure. Correspondingly, the algorithm will return output data to the caller in a data table or array structure. The delivered version will output data to a file to facilitate testing, and will need to be modified to pass the data to the system framework in place at the time of implementation.

The input data are assumed to be in calibrated scientific units of Watts/m^2, which are assumed to come from XRS Level 2 processing algorithms that produce 1-minute X-ray flux from the XRS-B (0.1-0.8 nm) channel. The XRS.07 algorithm assumes time values corresponding to the measurement data values are in units of the Julian Day (useful tor time series analysis), and the date and time (year, month, day, hour, and minute in UTC – useful for forecast operations), which is the time convention used in forecast operations. The cadence of data is expected to be monotonically increasing 1-minute averages. The time frame for the input data can vary, but it should be at least a 1-day ensemble of 1-minute samples to ensure the longest-duration flares can be accurately characterized, and to facilitate comparisons to other 1-day space weather products. More than 3 days of data may begin to negatively impact the algorithms performance. Furthermore, the algorithm assumes any missing data are flagged with a missing-value flag, e.g., -99999.0 W/m^2, or -1.0 x 10^5.

3.2 Processing Outline

Figure 5 below presents a notional flowchart of the XRS.07 algorithm, outlining the sequence of key operations. Briefly, the sequence is summarized as follows:

1. Form a data bin of real-time data (i.e., the "data-frame"), calculate the mean, median and standard deviation of the data frame for estimating signal noise,
2. Perform light smoothing of the data frame to reduce the effects of "signal noise" in the time series,
3. Determine if the flux exceeds 5.0 x 10^{-5} W/m^2, and if found, then signal the start of the flare (EVENT_START), and proceed to step 10,
4. Determine if a point of inflection has been reached in the slope of the data frame using the 2nd derivative of the data-frame (*where t=0 is a* **Equation 1**),
5. Ensure the mean of the last 3 points in a data-frame is some number of standard deviations above the mean of the first 3 data points in the data-frame,
6. If an inflection point has been reached and the data has increased sufficiently, continue processing the data frame to determine if the exponential increase reaches a high correlation coefficient by fitting an exponential function (**Equation 2**),
7. Ensure the maximum of the exponential function estimate lies above a certain percentage above the mean of the first 3 data points of the exponential fit,
8. If the inflection point has been reached, and the fitted exponential function has reached a high correlation coefficient, and the current data point lies above the estimated noise, flag the start of a flare event (EVENT_START),
9. Use the minimum of the fitted exponential function to estimate the pre-flare background,
10. Continue processing the time series to determine when the maximum has been reached, signaling the maximum of the flare (EVENT_PEAK),

11. Continue to process the time series until the end of the flare (EVENT_END) is reached by applying **Equation 3**,
12. Continue processing to determine if the flux has declined to the background level reached calculated in step 9.

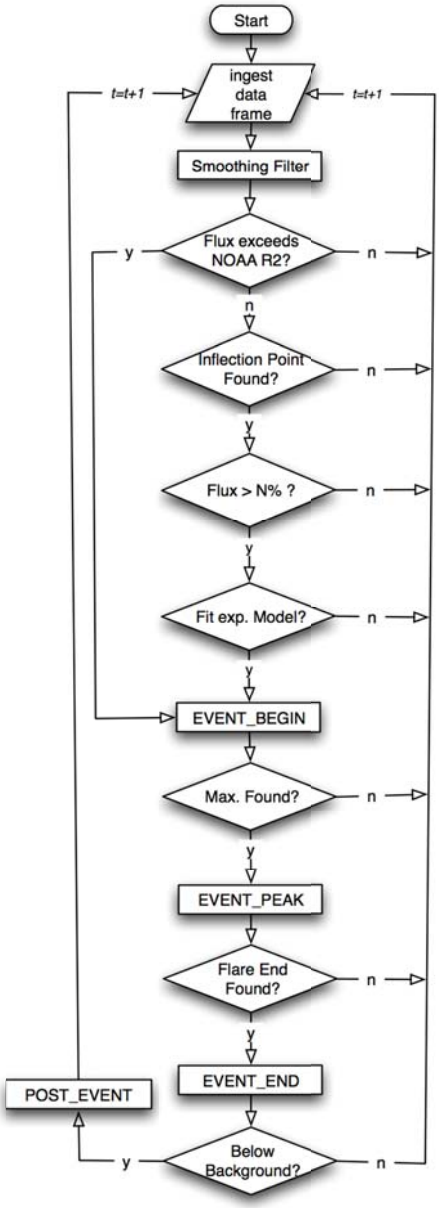

Figure 5. XRS.07 Algorithm Flowchart Overview.

At each EVENT_START, EVENT_PEAK, and EVENT_END, the algorithm increments the time pointer, ingesting another frame of data. When an EVENT_START has been set, the algorithm continues to step in time, searching for either and EVENT_PEAK or another EVENT_START, and if not found, repeatedly setting the status value to EVENT_RISE and returning for the next data-frame. Once an EVENT_PEAK has been detected, the algorithm continues setting the EVENT_DECLINE status values until either an EVENT_START or EVENT_END is detected. Once an EVENT_END has been reached, the algorithm sets the status values to MONITORING until a new EVENT_START has been detected. But if the flux reaches the background on the declining part of the vent, a POST_EVENT flag is set for that 1-minute step.

If there are any missing data within a data frame, the algorithm sets the IMPAIRED status until there are no missing data within the data frame, at which point the MONITORING flag is set. Normally, one or two missing data would not be a problem in time series analysis, but because the data frame is so small in this case, all data must be verified within a data frame as non-missing.

3.2.1 Mitigating Signal Noise and False-Positives

One of the challenges in developing the algorithm was mitigating the effects of signal noise, resulting in “false alarms” (or more accurately, false-positives). Additionally, “noisy” data can result in inaccurate identification of the flare peak or the flare end. Because the data-frame is so small, accurate statistics are difficult to achieve. However, small changes in pre-conditioning the data prior to a calculating an event property significantly reduces false-positives and missed event properties. Thus, the algorithm performs the following calculations:

1. Smooth the data in a data-frame with a small, simple boxcar filter prior to looking for the start of an event, using a parameter from the configuration table that specifies the size of the smoothing window. Typically a 3-minute window is adequate.
2. Calculate the mean of the first 3 and last 3 data values in a data-frame window to determine if the data are rising by some number of standard deviations, using the parameter from the configuration table
3. If a good fit is found between the data and the exponential model, verify that the exponential function is increasingly concave by taking the second derivative of the exponential fit, ensuring all 2nd derivative values are positive

4. In determining if the flare has risen by a percentage above background – specified in the configuration table - use the mean of the first 3 values of the fitted exponential to estimate the pre-flare background, comparing it to the flux at the inflection point, to see if it has risen above the estimated pre-flare background by the required percent increase.
5. In determining the flare maximum, use a parameter in the configuration table that specifies the size of the window in determining the maximum, smoothing a data-frame window spanning a potential maximum, then use the maximum in the smoothed frame to determine when the maximum occurred, then use the flux at that point to estimate the flare class output to the Event Status Output Table
6. In determining the event end (½ max. point), use the median of the most recent 3 values in the data-frame.
7. In determining the percent increase above the background (EVENT_START), and in determining the EVENT_END, use the logarithmic conversions (**Equation 3** and **Equation**).

3.3 Algorithm Input

- Data:
  - $XRS_{1\text{-}8}$ = An epoch of 1-minute averages of the integrated spectrum in calibrated science units. It is assumed the data in the epoch are increasing in time monotonically, and missing data is flagged (e.g., -99999.0 W/m^2, or -1.0 x 10^5)
  - Timestamp of $XRS_{1\text{-}8}$ values, in Julian Days or the year, month, day, hour, minute, and second in UTC.

- Level 1b Configuration parameters, stored as a look-up table (see 3.3.2 Configuration Parameters).

3.3.1 Primary Sensor Data

GOES-R XRS X-ray flux, 01.-0.8 nm integrated flux, 1-minute averages.

3.3.2 Configuration Parameters

The configuration data will be in a look-up table. The parameters specified in the lookup table will need to be determined post-launch, in order to determine the statistical properties of the data that are unique to the instrument's performance. For data that have good signal-to-noise properties, the initial defaults shown

below should be sufficient. If the signal-to-noise ratio is poor, the parameters will need to be increased. In either case, iteratively modifying the configuration parameters will improve performance. In **Table 7**, the items marked in bold are the most important: small changes will significantly change the performance of the algorithm. The other parameters, once set, will probably not need to change.

Table 7. Recommended Configuration Parameters

Parameter	**Recommended** (based on GOES-15)	**Expected Range**
Data frame size	**9 minutes**	**7-13 minutes**
Percent above background criteria	**22.5%**	**0.15% – 0.35%**
Minimum correlation coefficient criteria	0.925	9.0 – 9.9
Number of standard deviations above background criteria	1	1-1.5
Size of smoothing window	3 minutes	3-5 minutes
Size of data frame used to determine event maximum	7 minutes	5-7 minutes
The minimum amount of absolute flux the inflection point must pass to be identified as an event beginning	1.0×10^{-7} W/m^2	1.0×10^{-7} W/m^2 - 1.0×10^{-8} W/m^2
The lower limit by which flux is physically valid, below which the Status Flag is set to IMPAIRED	9.0×10^{-8} W/m^2	1.0×10^{-9} W/m^2 – 9.9×10^{-8} W/m^2
The number of minutes to wait after detecting a flare start before considering another event start	8 minutes	5 – 10 minutes
Missing-value flag	-1.0×10^{5}	(must be < 0.0)

3.4 Theoretical Description

The event detection algorithm defined here is intended to significantly improve on the algorithm currently in use at NOAA/SWPC, in that it is a “hands-off” real-time process that will detect the large majority of flare conditions. It detects the onset of an event as rapidly as possible (i.e., the event is detected prior to the flare reached it’s maximum), while minimizing “false-positives” (i.e., miss-identifying a

minor event as a flare) and “false-negatives” (i.e., not detecting the onset of a flare).

3.4.1 Physics of the Problem

Solar x-ray flux comes primarily from a two sources: (1) numerous small bright points over the entire disk which are unrelated to active regions (sometimes called “micro-flares”), (2) active regions and coronal loops associated with active regions. The numerous bright points are thought to provide a background component to the time series, but the active region sources contribute the majority of x-ray flux, especially when a flare occurs. Multiple active regions will result in a time series that contains all these sources, and when solar activity is high, multiple flares can occur in rapid sequence, resulting in a complex time series, particularly when there are “double-ribbon” flares from one active region.

Traditionally, rapid rise of the flare from the onset has been referred to as the “impulsive” phase, and the gradual decline as the “gradual” phase. The impulsive phase of the flare will almost always exhibit an exponential increase during which the data curve will continually increase in the rate of change, but at some point the impulsive phase will exhibit a decreasing rate of change, and at that point one can determine the inflection point in the data curve.

Flare event detection can be very problematic when there are multiple sources of x-ray flux, as determining a background by which an increase can be detected is complicated by rapidly-varying contributions from other events in progress. Furthermore, while the rate of increase during the impulsive phase is typically a rapid exponential rise within 1-5 minutes, but more gradual flaring can also occur on the order of 5-60 minutes (in rare instances, flares can last as long as about 8 hours). The flare event detection algorithm is designed to address all of these instances, although solar x-ray activity can behave in a highly variable fashion causing the algorithm to misidentify the event status (e.g., flares that gradually rise to high flux levels over approximately 60-120 minutes, or when a flare reaches a maximum from the background in under 1-3 minutes, both of which are fairly rare instances.

3.4.2 Mathematical Description

The following is a brief description of the algorithm. The algorithm will first perform some pre-processing of the input data to ensure it contains no missing values, and to eliminate some of the noise in the time series. It does this by slightly smoothing the data with a running boxcar filter to remove the small high-

frequency components (this is an adjustable parameter, but typically is only 3-5 minutes long). It is assumed the input data is monotonically increasing in time.

The first key part of the algorithm is detecting the beginning of a flare. In addition to identifying when the flux increases by a certain percentage, the algorithm looks for the point of inflection, which is where the maximum in 2nd derivative is found, setting a flag that will cause the second equation to be executed.

$$EVENT_BEGIN(t_i) = Max\left[\frac{d^2\Phi}{dt^2}\right]$$

where
t=0 to n

Equation 1. The first equation used to detect the onset of a flare.

Figure 6 illustrates this, showing the evolution of a typical flare (top panel). During the early onset of the flare, the 2nd derivative (bottom panel) reaches a maximum value, identifying a point of inflection. Also illustrated with a short bold line, is a simple exponential model fitted to the data, which is discussed below.

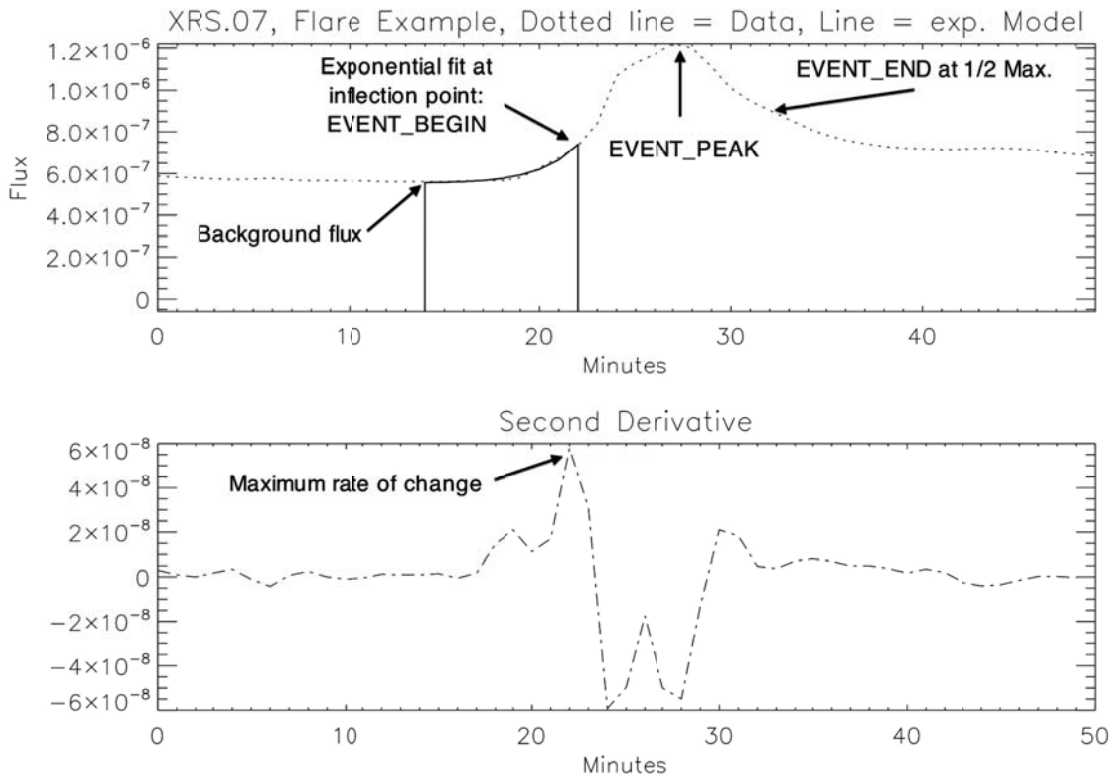

Figure 6. Event identification concept.

However, there can be many points of inflection in a time series of x-ray flux, so a second key step is to see if the time series begins to demonstrate the unique property of an exponential rise in flux during the onset of a flare, often called the "impulsive" phase of a flare. This is done by solving the following equation, searching for the highest correlation coefficient within the data frame.

$$\Phi_{imp}(t) = a \bullet \Phi(t) \bullet e^{\left(b \bullet \Phi(t)\right)} + c$$

Equation 2. The exponential model used to indentify the start of the impulsive phase of a flare.

When finds the coefficients that result in the highest correlation coefficient, the EVENT_START flag is set, and the algorithm then proceeds to watch for the maximum of the flare, or another start of a flare before the maximum is reached.

Combined with the initial criteria that the data must increase by a certain percentage, Equations 1 and 2 can be jointly used to separate the “signal” in the time series above a “noisy” background.

Determining the end of a flare is problematic, partly because during declining phase of the flare, another flare may begin before the earlier flare reaches it’s event end. Currently, at SWPC the end of the flare is when the flare decreases by ½ of the maximum flux minus the background level: this is a practical definition most useful for forecasters in operations.

$$\Phi_{end}(t) = \frac{\left(\Phi_{\max} - \Phi_{\text{background}}\right)}{2}$$

Equation 3. The equation used to identify a flare event end.

But **Equation 3** begs the question: how is the x-ray background best determined? This can be difficult to estimate; for example, should an hourly average be used to estimate a background, or a shorter time interval? In any case, significant signal noise or rapidly repeating flares can result in a much too high background estimate, significantly hindering the ability of an algorithm to detect or characterize a flare. By fitting an exponential model to the initial rise of a flare, and using it’s minimum value, a more accurate background can be estimated that is far less susceptible to rapid flaring or signal noise. However, the exponential fit is not 100% accurate, and the background can still be in error by up to about +-20% in some cases where the pre-flare data has significant signal noise or the flare rises from min to max in under 1-3 minutes. Thus, the algorithm will follow the following sequence to determine the EVENT_END:

1. After the EVENT_PEAK has been reached, search for the ½ maximum (EVENT_END), setting the flag that indicates the flare has ended: this is an operational definition consistent with legacy practices.
2. Next, search for the point at which the flare has decayed to it’s pre-event background (POST_EVENT), which is determined by the minimum value of the exponential fit shown in Equation 2.
3. If either (1) or (2) has not been reached before another flare has started, the algorithm will simply report the beginning of a new flare, and the EVENT_END will not have been set. However, the prior flare has effectively ended at that point.

Equation 3 also can be applied to the determination of the EVENT_START, by applying it to the event background and percentage increase of the fitted exponential model at the inflection point.

$$Percent_Increase = \frac{\left(100 * \log(\Phi_{\inf} * 10^{10}) - 100 * \log(\Phi_{background} * 10^{10})\right)}{100 * \left(\log(\Phi_{\inf} * 10^{10})\right)}$$

Equation 4. Determining the percent increase of the exponential fit.

3.4.3 Algorithm Output

The initial output requirements were:

1. The flare event detection time T_S
2. The flare maximum time T_M
3. The flare end time T_E

As discussed above, during development it was discovered the algorithm can also estimate the pre-flare background using **Equation 2.** For isolated flares, the integrated flux from the pre-flare background to the time the flare decays to that pre-flare background is useful for other operational and scientific purposes, such as determining the total energy input of the flare to the D-region of the ionosphere.

4.0 TEST DATA SETS AND OUTPUTS

The algorithm must address both solar maximum conditions, when there are large multiple flares in progress, and solar minimum conditions when there are smaller flares above a low background with numerous micro-flares. Three datasets have been assembled for development and testing periods:

Table 8. Study epochs used for development and testing.

Epoch Start Time	Epoch End Time	Note
Feb. 10, 2011	Mar. 21, 2011	Recent moderate solar activity
Oct. 25, 2010	Nov. 10, 2010	Recent low solar activity

Oct. 25, 2003	Nov. 10, 2003	High solar activity

The 2010 and 2011 epochs were selected so that the XRS07 epochs coincide with the times SDO/EVE data are available; this will provide a useful baseline for the EUVS.04 event detection algorithm development, and contains the low-medium levels of solar activity for a qualitative algorithm performance evaluation. The Oct 25, 2003 to Nov 10, 2003 was selected because that epoch demonstrates the some of the most active in x-ray events during solar cycle 23.

4.1 Simulated/Proxy Input Data Sets

Test data sets will be collected from historical GOES-12 and GOES-15 XRS measurements. These data are from the primary operational GOES XRS measurements, thus the data represent typical real-time conditions and event properties. The Feb 10 – Mar 21, 2011, and the Oct 25 – Nov 10, 2010 study epochs were used in the algorithm development. The Oct 25 – Nov 10, 2003 will be used to evaluate the algorithm performance.

4.2 Output from Simulated/Proxy Inputs Data Sets

Output from the algorithm will produce an ordered data list with the date/time, Julian Day, flux, an Event Status Flag (0-9), an Event Status Flag. **Table 9** below illustrates what this table looks like. At each minute, a new line is written to this output table with date/time, Julian Day, Flux, and the Event Status. All date/times are in UTC.

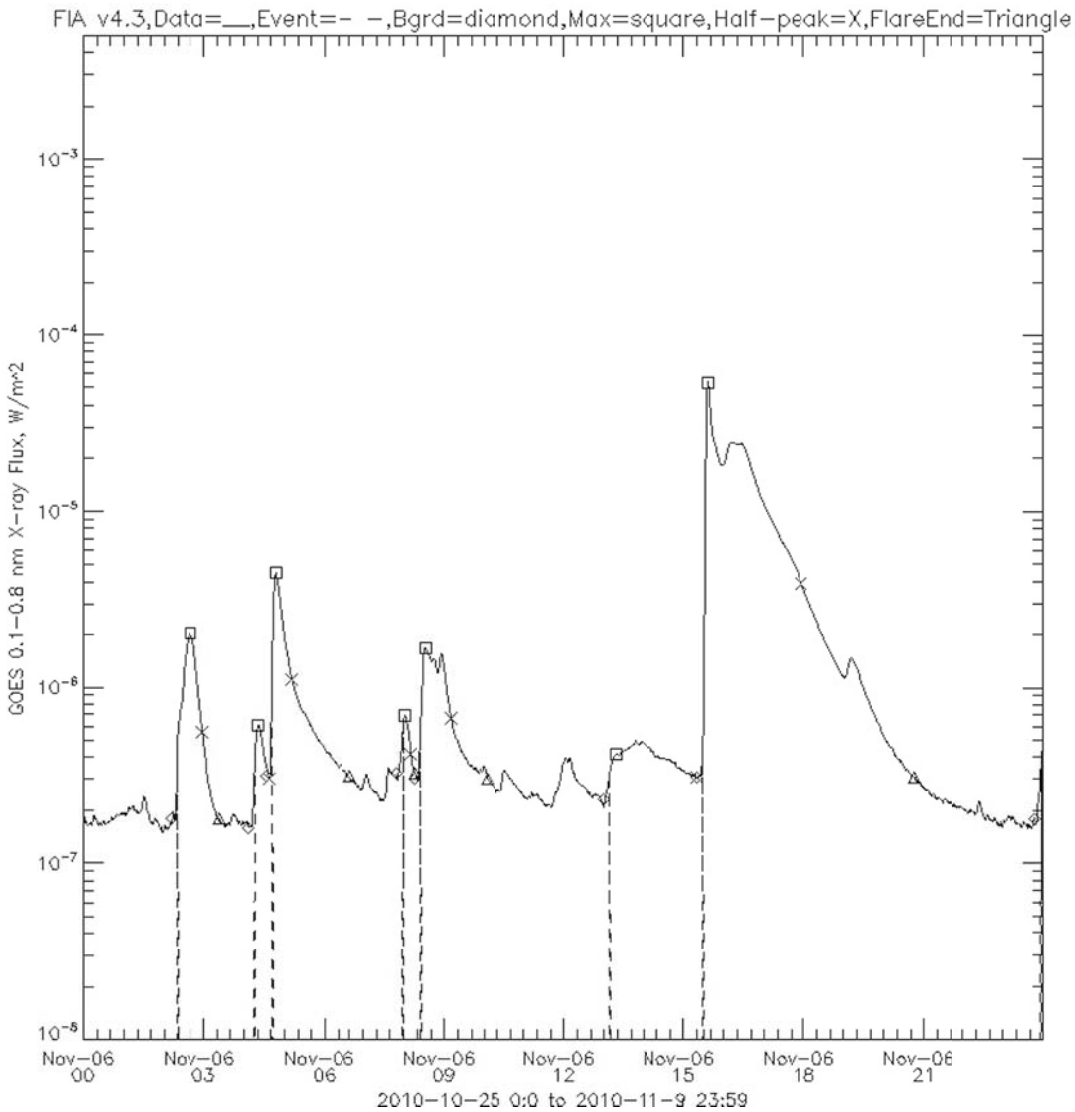

Figure 7. Example of algorithm performance in detecting flares, Nov. 6, 2010

In the example in Figure 7, the algorithm parameters were adjusted to reduce false alarms. Thus, the small “micro-flares” were not flagged, but one legitimate flare was overlooked by the algorithm. This illustrates the unavoidable trade-off between minimizing false positives, at the expense of increased lag times between the event start and flare maximum and missed events.

To illustrate what the algorithm outputs as a flare event evolves, consider the small flare preceding the large event near hour 08 UT in Figure 7. The output of the algorithm is shown in **Table 10**, where within the span of 20 minutes, the flare begins, reaches the peak, declines to ½ it's maximum value, then finally declining to the pre-flare background. Note that for all the event status flags, the algorithm's output lags the actual occurrence of an event by about ½ of the data-frame (the data-frame is 9 minutes in this case). In this example, the maximum was detected 4 minutes after it actually occurred.

Table 9. Real-time Status Output Table example.

YYYY	MM	DD	HH	MM	JD	Flux	Event Status
2010	11	06	07	58	2455506.831944	5.239E-07	MONITORING
2010	11	06	07	59	2455506.832639	6.017E-07	EVENT_START
2010	11	06	08	00	2455506.833333	6.675E-07	EVENT_RISE
2010	11	06	08	01	2455506.834028	6.876E-07	EVENT_RISE
2010	11	06	08	02	2455506.834722	6.851E-07	EVENT_RISE
2010	11	06	08	03	2455506.835417	6.682E-07	EVENT_RISE
2010	11	06	08	04	2455506.836111	6.442E-07	EVENT_RISE
2010	11	06	08	05	2455506.836806	6.063E-07	EVENT_PEAK
2010	11	06	08	06	2455506.837500	5.757E-07	EVENT_DECLINE
2010	11	06	08	07	2455506.838194	5.542E-07	EVENT_DECLINE
2010	11	06	08	08	2455506.838889	5.116E-07	EVENT_DECLINE
2010	11	06	08	09	2455506.839583	4.744E-07	EVENT_DECLINE
2010	11	06	08	10	2455506.840278	4.477E-07	EVENT_DECLINE
2010	11	06	08	11	2455506.840972	4.202E-07	EVENT_END
2010	11	06	08	12	2455506.841667	3.960E-07	MONITORING
2010	11	06	08	13	2455506.842361	3.668E-07	MONITORING
2010	11	06	08	14	2455506.843056	3.492E-07	MONITORING
2010	11	06	08	15	2455506.843750	3.380E-07	MONITORING
2010	11	06	08	16	2455506.844444	3.259E-07	MONITORING
2010	11	06	08	17	2455506.845139	3.233E-07	POST_EVENT
2010	11	06	08	18	2455506.845833	3.137E-07	MONITORING

To address this latency, a second output table - called the Event Status Output Table - is produced by the algorithm, which reports the flare start, maximum, end, and when it reaches the pre-flare background (post-event) at the times they actually occurred. Additionally, it reports on what the background flux was prior to the event start, the flare class at EVENT_PEAK, the integrated flux between EVENT_START and EVENT_END at the EVENT_END in an Auxiliary column as shown in **Table 10**. There is no additional field for POST_EVENT.

Table 10. Event Status Output Table example.

YYYY	MM	DD	HH	MM	JD	Flux	Event Status	Aux.

```
---- -- -- -- --  -------------- --------- ------------ ---------
2010 11 06 07 58 2455506.831944  6.017E-07 EVENT_START  0.325E-06
2010 11 06 08 01 2455506.834722  6.851E-07 EVENT_PEAK    B 6.9
2010 11 06 08 10 2455506.840278  4.202E-07 EVENT_END      0.102E-04
2010 11 06 08 13 2455506.842361  3.233E-07 POST_EVENT
```

4.2.1 Precisions and Accuracy Estimates

The precision of XRS measurements is determined by the precision of the instrument. The accuracy of the algorithm is related to the time the algorithm detects the onset of the flare prior to the flare maximum. The algorithm performance will be compared to either the edited event lists from NOAA/SWPC, or to a manually edited list created by visual inspection. In order to gain sufficient statistics to evaluate the performance, the testing will be done on a time series the contains over 100 C, M, and X class flares.

4.2.2 Error Budget

As discussed earlier, there are a number of trade-offs between the event detection latency, event detection sensitivity, false-positives, and false-negatives. Consequently, error estimates depend on the adjusted parameters in the configuration (See section 3.3.2 Configuration Parameters). These parameters will need to be adjusted to account for the signal-to-noise properties of the data. Based on the performance of the algorithm processing historical GOES-15 XRS 1-minute data, and using the configuration parameters shown in **Table 7**, the best compromise yielded the approximate error estimates is shown in **Error! Reference source not found.Table 11**.

Table 11. Error budget estimates, assuming a 9-minute data-frame size.

Components	**Error Estimate**
Absolute x-ray flux, 1-minute averages	+- 10%
Pre-flare background flux	+- 20%
Pre-flare background time	+- 4 minutes
Flare maximum flux	+- 10%
Flare maximum time	+ 1-4 minutes
Flux at EVENT_END	+- 10%
Time of EVENT_END	+ 1-4 minutes
Flux at POST_EVENT	+- 15%
Time of POST_EVENT	+ 1-15 minutes
Percentage of missed B class flares	30%

Percentage of missed C to M5 class flares	5%
Percentage of missed M5 to X class flares	<1%
Percentage of false positives B and C class flares	20%
Percentage of false positives C to M5 class flares	5%
Percentage of false positives, M5 to X class flares	<1%

5.0 PRACTICAL CONSIDERATIONS

One potential change to the XRS.07 algorithm that may be required is if the 1-minute data has redefined inputs from what are described in this document. For example, if the data are not increasing in time monotonically, the algorithm may fail to correctly identify event characteristics or report false positives (Although the algorithm will proceed without crashing). Similarly, if sudden decreases in x-ray flux occurs (e.g., during an eclipse, or other outages), the algorithm may fail to identify an event in progress when data start after the outage.

However, the parameters that define data-frame sizes, percent above background, etc. (3.2.1) are dependent on the signal-to-noise properties of the data. There is no apparent method to determine computationally how to adjust run-time parameters from the statistical properties of the data. Thus, new data that have a varying signal-to-noise ratio (e.g., a new instrument, instrument degradation, etc.), the algorithm will need to be adjusted by manually varying the parameters in the lookup table interactively, using a large sample size that contains approximately 100 flare events.

5.1 Numerical Computation Considerations

Early in the algorithm development it was discovered that there is a trade off between rapidly detecting all potential flares (the sensitivity), resulting in increased false-positives, or on the other hand, or reducing the sensitivity so that only C to X-class flares are detected (accuracy), resulting in more false negatives. NOAA/SWPC indicated that in general, accuracy is more important than sensitivity. In any case, the balance between accuracy and sensitivity can be more objectively determined in testing the algorithm's performance with a large sample size.

The algorithm is not computationally expensive, and it will easily complete a cycle of calculations in under one minute, assuming the data arrays are on the order of one day. Single-precision flux data is adequate (but Julian Day should be double-precision). One day of 1-minute values are chosen to ensure extreme

long-duration events (on the order of 8 hours) are tracked from the beginning to the event end (POST_EVENT).

5.2 Programming and Procedural Considerations

The delivered XRS.07 algorithm will be written in Fortran. The system framework the algorithm will be running under is undetermined as yet, so the output of the algorithm will write the results to files. When the algorithm is finally implemented, the output will need to be passes back through the subroutine to the caller, or simply left as-is, depending on final implementation requirements.

5.3 Quality Assessment and Diagnostics

The key goals for testing the algorithm are (Table 3):

- Ensure the algorithm identifies 80% of all B class flares,
- Ensure the algorithm identifies 90% of all C class flares,
- Ensure the algorithm identifies 99% of all M and X class flares,
- Ensure the algorithm detects the onset of a flare before flare maximum,
- Ensure the algorithm performs all calculations within 60 seconds
- The algorithm does not result in a “hung” condition or it does not result in any “memory leaks”

These goals can be addressed by developing a test-bed program that encapsulates the algorithm, reading from data files the simulated input data, then piping the data to the algorithm. The output files from the algorithm can then be examined for performance. Test data is from historical archives of GOES XRS 1-minute data can compared to historical edited event lists from NOAA/SWPC, although in practice, the NOAA tables are not 100% accurate, and visual inspection is the most reliable.

It is recognized by NOAA/SWPC that these performance goals are an approximation, and that there are trade-offs between accuracy and latency that need to be evaluated during development and testing to find the best combinations between the parameters (see **Table 7**). NOAA/SWPC has indicated that reducing false-positives and false-negatives take priority over reducing latency (i.e., how rapidly the algorithm can detect the flare before it reaches it’s maximum). And, as noted before, the performance of the instrument during the mission lifetime, i.e., the signal-noise ratio, is the key property that determines the performance of the algorithm.

In initial testing during development, all of the design goals were met (Table 3), and the initial test results were used to develop the error budget. Two of the most desired goals – detecting a flare as early as possible (e.g., 4 minutes after start) and detecting nearly all C, M, and X-class flares – were accomplished. Indeed, for large flares that took up to about 30 minutes, the algorithm detected the flare start as early as 20 minutes prior to flare maximum. These results will be described in detail in the test plan and user guide.

5.4 Exception Handling

The algorithm shall trap all exceptions, and in the event significant data is missing or out of range, the algorithm will assign an "IMPAIRED" status value (**Table 4**). It is assumed the data meet the criteria specified in 6.0 ASSUMPTIONS AND LIMITATIONS.

5.5 Algorithm Validation

The XRS.07 algorithm will be tested with 4 data sets from GOES-12 and GOES-15 measurements from data archives (**Table 9**). During development and initial testing, the periods during 2011, 2010, and 2003 will be used to evaluate performance for B, C, M, and X-class flares.

6.0 ASSUMPTIONS AND LIMITATIONS

1. It is assumed that the XRS.07 algorithm inputs will be:
    a. A minimum of 1,440 XRS-B 1-minute averages, monotonically increasing in time, with missing data flagged with a missing-value flag, e.g., -1.0×10^{-5}
    b. Data outages (e.g., during solar eclipse) are flagged with missing-value flags
    c. The data are above a minimum value representative of valid instrument performance, e.g., 1.0×10^{-9}
    d. A-class flares (1.0×10^{-8} to 1.0×10^{-7} are not to be considered
    e. All data within a data frame are not flagged as missing; if there are missing data, the algorithm will set the IMPAIRED status flag, clearing any prior status flag, until all data are present within the data frame, at which point the status returns to MONITORING

The assumption that the data are ingested as a 1,440 minute data block (i.e., one day) is based on two considerations: (1) Very long-duration events (greater than

8 hours) should be captured in their entirety, and (2), other GOES XRS products (e.g., the daily background flux) use 1,440 1-minute data blocks, and maintaining that convention allows for other practical and scientific applications of the algorithm's outputs.

6.1 Performance

The lifecycle of the algorithm (i.e., time to completed calculations from receipt of input to the output of data) shall be less than 60 seconds. Based on the performance of the algorithm, this can be achieved in a fraction of the time.

The algorithm design goals were to detect a minimum of 80% of B class flares, 90% of C class flares, and 99% of M and X-class flares. Also, the start of the flare should detect the initiation of the flare at least 1-4 minutes prior to flare maximum. NOAA/SWPC clarified that these are goals, and may need to be adjusted after testing. Also clarified was given that there will be a trade-off between the sensitivity of the algorithm and false-positives, preference should be given to minimizing false-positives. Nevertheless, preliminary testing of over 200 flares indicates that all of these performance goals have been achieved or exceeded. Most notably, the average time before a flare maximum the algorithm detected the flare was 9 minutes.

6.2 Assumed Sensor Performance

It is assumed the XRS instrument will operate within design requirements as specified in EXISPORD81 (417-R-EXISPORD-0116, 2008).

6.3 Pre-Planned Product Improvements

There are no pre-planned product improvements at this time.

7.0 REFERENCES

Tobiska, W.K. and S.D. Bouwer, "Solar flare evolution model for operational users", 2005 *Ionospheric Effects Symposium*, ed. J.M. Goodman, JMG Associates, 76, 2005

Bouwer, S.D, et. al., "A Summary of 1-8A Measurements from the SMS and GOES Satellites, 1977-1981", NOAA Tech. Memo. ERL SEL-62, July 1982.

Bouwer, S. Dave, "A Summary of SOLAR 0.1-0.8nm X-ray Measurements From the GOES Satellies,1986-2004", Internal SET report, 2006. http://www.spacewx.com/pdf/SET_TR2006_002.pdf

Chamberlin, P. C., F. G. Eparvier, A. R. Jones, and T. N. Woods, “Next Generation X-Ray Sensors (XRS) for the NOAA GOES-R Series Satellites”, SPIE Proceedings, in preparation, 2009.

Garcia, H. A., “Temperature and emission measure from GOES soft X-ray measurements, Solar Physics, 154, 275, 1994.

Woods, T. N., P. C. Chamberlin, W. K. Peterson, R. R. Meier, P. G. Richards, D. J. Strickland, G. Lu, L. Qian, S. C. Solomon, B. A. Iijima, A. J. Mannucci, and B. T. Tsurutani, “XUV Photometer System (XPS): Improved irradiance algorithm using CHIANTI spectral models”, Solar Physics, 249, doi 10.1007/s11207-008-9196-6, 2008

NASA/GOES-R/Code 417, “GOES-R EUVS XRS Irradiance Sensors (EXIS), Performance and Operational Requirements Document (PORD)”, Document Ref: 417-R-EXISPORD-0116, Vers. 2.3, June 25, 2008.